Available online at www.sciencedirect.com
SCIENCE DIRECT®

Journal of the European Ceramic Society 24 (2004) 3155–3168

www.elsevier.com/locate/jeurceramsoc

Rheological study of a talc-based paste for extrusion-granulation

P.J. Martin[a], D.I. Wilson[a,*], P.E. Bonnett[b]

[a]*Department of Chemical Engineering, University of Cambridge, Pembroke Street, Cambridge CB2 1TP, UK*
[b]*Process Studies Group, Syngenta, Huddersfield Manufacturing Centre, Huddersfield HD2 1FF, UK*

Received 30 May 2003; received in revised form 27 October 2003; accepted 1 November 2003

Abstract

The rheological behaviour of an industrial talc-based paste featuring a solids volume fraction of 0.49 in a viscous aqueous surfactant solution was studied using a form of capillary rheometry. Standard approaches for determining wall slip velocities yielded non-physical results, although the data could be correlated using the Jastrzebski wall slip condition. The material was also characterised using the Benbow–Bridgwater approach and showed variations with die land diameter which could not be correlated using simple corrections. The parameters obtained featured an accuracy of ±20%. Density measurements indicated that dilation and liquid-phase migration were important features of the flow, and that the stresses are chiefly borne by the liquid-phase. The flow behaviour is interpreted in terms of the component properties: the difficulty in rheological characterisation is attributed to shear-induced re-orientation of the talc platelets during flow.

Keywords: Extrusion; Platelets; Rheology; Silicates; Suspensions; Talc

1. Introduction

A paste can be described as a very dense suspension of solid particles in a viscous liquid-phase with sufficiently high solids volume fraction to render the material stiff, but readily deformable. Typically, a paste possesses an apparent yield stress which is sufficient to prevent deformation of the material under gravity. Hence, it may be easily formed into a desired shape, and will retain this shape until further processing. Extrusion is commonly utilised to achieve the desired shape, and finds application in the production of a range of goods, including catalyst supports, ceramic items, foods and electronic components. Rheological studies of pastes are required to develop novel extrusion applications, and to improve product quality and process optimisation.[1–4]

Powdered talc (magnesium silicate) is used in many extruded products. It may be added to bulk out a material, to modify its flow properties, or to modify the final product properties. One major use is as a filler in extruded thermoplastics, where it is added at up to 40 wt.%.[5] This paper is concerned with the use of talc in extruded agrochemical products. The concentrated active ingredients of the agrochemical (insecticides, herbicides, fungicides) must be contained in a form which may easily be stored, transported and then diluted in water to form a solution for spraying. Water dispersible granules (WDGs) are one product form which satisfies these basic criteria. WDGs are manufactured by mixing together talc and water to make a paste. Other ingredients may be added, for example harborlite (milled perlite) and surfactants which improve dispersibility. A summary of the key constituents of a typical talc-based WDG paste is given in Table 1. Fig. 1 shows a flowsheet for an industrial WDG production process: cylindrical granules are formed by extrusion of the paste through a screen (extrusion-granulation), then dried and packaged. The paste velocities within the extruder may vary between 0.003 m/s and 0.3 m/s, and the paste flow undergoes area reduction factors of up to 20.[6]

Understanding the relationships between paste formulation, processing conditions and the final product properties would enable better quality control and product design. The large number of parameters involved makes a generalised scientific codification of this process difficult to express, although some aspects have been covered.[7,8]

* Corresponding author. Tel.: +44-1223-334777; fax: +44-1223-334796.
E-mail address: ian_wilson@cheng.cam.ac.uk (D.I. Wilson).

0955-2219/$ - see front matter © 2003 Elsevier Ltd. All rights reserved.
doi:10.1016/j.jeurceramsoc.2003.11.003

Nomenclature

D	die land diameter
D_0	barrel diameter
K	Herschel–Bulkley shear rate coefficient
L	die land length
m	Benbow–Bridgwater die entry velocity index
n	Benbow–Bridgwater wall slip velocity index
P	extrusion pressure
P_1	component of extrusion pressure associated with die entry flow
P_2	component of extrusion pressure associated with die land flow
Q	volumetric flow rate
r	capillary radial co-ordinate
R^2	coefficient of correlation
V	mean extrudate velocity
V_p	piston velocity
V_{shear}	velocity associated with bulk shear
V_{slip}	wall slip velocity
w	mass fraction Morwet
x	capillary length co-ordinate
Y	die entry yielding stress
Greek	
α	Benbow–Bridgwater die entry velocity coefficient
β	Benbow–Bridgwater wall slip velocity coefficient
β_c	Jastrzebski wall slip velocity coefficient
$\dot{\gamma}$	shear rate
$\dot{\gamma}_A$	apparent shear rate
λ	Herschel–Bulkley shear rate index
μ	apparent viscosity
ρ	density
σ_0	Benbow–Bridgwater die entry yield stress term
τ	shear stress
τ_w	wall shear stress
τ_y	Herschel–Bulkley yield shear stress
τ_0	Benbow–Bridgwater wall yield shear stress

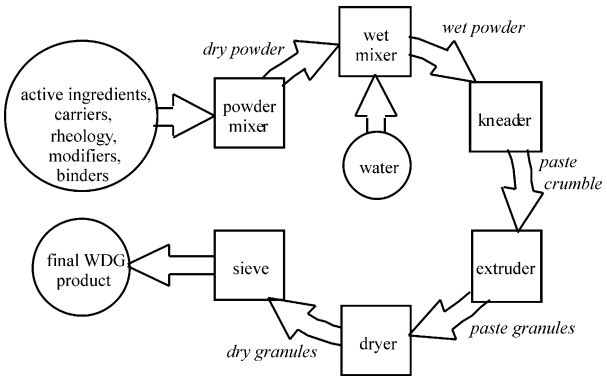

Fig. 1. Schematic of an industrial WDG production process.

This paper describes the rheological characterisation of a model talc-based paste, which mimics an industrial system, and relates this in a basic way to its formulation. The rheological characterisation is performed over a range of flow conditions, and is thus appropriate for further studies examining the flow of paste within an actual extrusion-granulator.[6] As extruder flow conditions (for example, stresses generated causing paste compaction and shear) determine to a large extent the final granule properties, this paper helps to link paste formulation and extruder operating conditions to the final WDG.

For convenience, the rheology of pastes are often described as a single-phase continuum using a single constitutive equation. Their possession of an apparent yield stress, and their tendency to display a power law rate dependence, often makes the Herschel–Bulkley constitutive model[9] a suitable choice. Expressed in its one dimensional form, this relates the shear stress, τ, to the steady shear rate, $\dot{\gamma}$, by:

$$\tau = \tau_y + K\dot{\gamma}^{\lambda} \qquad \tau \geqslant \tau_y \tag{1}$$

$$\dot{\gamma} = 0 \qquad \tau < \tau_y \tag{2}$$

where τ_y is the yield stress and the parameters K and λ describe the rate dependence. Although the bulk material may be approximated as a single phase, the effects of phase migration, i.e. two-phase behaviour, are often significant. Of particular importance is shear-induced

Table 1
Model paste key constituents and formulation

Constituent	Description	Function	Wt. frac.	Source
Micro-Talc AT Extra	Magnesium silicate	Soft bulk material—easily dispersible	0.708	Norwegian Talc (UK) Ltd.
Harborlite S200Z	Milled perlite—siliceous volcanic glass	Hard bulk material—easily dispersible	Not used	
Morwet EFW	Anionic surfactant	Binder/rheology modifier/dispersant	0.0833	Petrochemicals Company Ltd., Ft. Worth, Texas, USA
Morwet D425	Surfactant—sodium naphthalene sulphonate-formaldehyde condensate	Binder/rheology modifier/dispersant	0.0417	Witco Corporation, Houston, Texas, USA
Water	Reverse osmosis water	Solvent/liquid-phase	0.167	Elgastat Prima 4, Elga Ltd., High Wycombe, UK

migration of the liquid-phase at the interface between the paste and the channel wall.[10] This creates a liquid-phase rich layer at the interface, which might typically have a thickness of one particle diameter.[11] This interface layer may act as a lubricant and allow the paste to slip against the wall. Precise measurements of the interface layer thickness in pastes have not been reported; usually the shear stress acting on the paste at the wall, τ_w, is simply related to the slip velocity, V_{slip}, by an expression such as that proposed by Benbow and Bridgwater:[12]

$$\tau_w = \tau_0 + \beta V_{slip}^n \quad (3)$$

where τ_0 is a yield stress, which may occur when fine suspensions of clays are present in the interface layer, and β and n describe the rate dependence.

For extrusion-granulation systems, it is most appropriate to choose a characterisation technique based on extrusional flow. Axisymmetric ram extrusion through a square entry, parallel-sided die is a standard experimental technique for paste characterisation.[12] Fig. 2 shows a cross-section of such a ram extruder with barrel diameter D_0, die land diameter D and die land length L. The ram forces paste to flow with a volumetric rate Q from the barrel into the die land. The region upstream of the constriction, where bulk deformation and extensional flow occurs, is known as the die entry region, and sometimes a static zone of paste forms in the corner of this region. The die entry region may extend slightly into the die land, but usually only to a negligible extent. The flow within the die land is usually pure shear and laminar, with mean velocity V; it may be considered as capillary flow, and is often plug flow owing to extensive wall slip. The force required to extrude the material through the die is expressed as an average 'extrusion pressure', P.

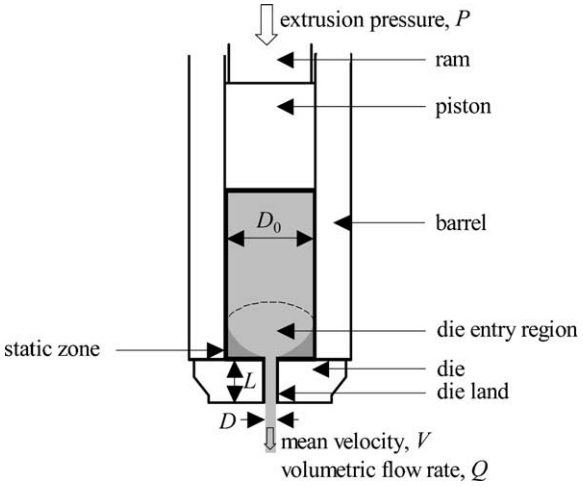

Fig. 2. Cross-section of a ram extruder with a square entry die.

1.1. Capillary flow analysis

When paste undergoes shearing in the die land, three factors may contribute to the net flow; wall slip, shearing and plug flow. These are illustrated in Fig. 3, where the flow is in the axial x-direction. The net velocity with respect to the die at a radial distance r from the axis is composed of two terms: namely V_{slip}, associated with flow due to wall slip, and a superficial velocity, V_{shear}, associated with bulk shear. Plug flow can still occur in the core where the local shear stress τ_{rx} is less than the paste yield shear stress τ_y.

An analysis of this flow for power law fluids yields the Weissenberg–Rabinowitsch equation,[13] and this was extended by Mooney[14] for Herschel–Bulkley materials, which can exhibit wall slip, to give:

$$\frac{32Q}{\pi D^3} = \frac{8}{D} V_{slip} + \frac{4}{\tau_w^3} \int_{\tau_y}^{\tau_w} \left(\frac{\tau - \tau_y}{K} \right)^{1/\lambda} \tau^2 d\tau \quad (4)$$

For a Newtonian fluid the right hand side of this expression reduces to τ_w/K; correspondingly the left hand term, $32Q/\pi D^3$, is sometimes called the apparent shear rate, $\dot{\gamma}_A$.

In practice, a series of experiments are conducted at constant flow rate and capillary diameter with a variety of L/D ratios. It is assumed that the entry pressure drop is independent of the absolute pressure, and that the wall shear stress is constant along the length of the capillary. Bagley plots[15] are constructed, from which the wall shear stress can be related to each flow rate and capillary diameter used. These data are used to construct a series of Mooney plots which indicate the paste slip velocities over the corresponding wall shear stresses (assuming that the slip velocity is exclusively a function of the wall shear stress).

1.2. Die entry analysis

The plastic nature of pastes means that they often undergo total slip at the wall and flow as a plug through the die land. In this case the rheological behaviour may be characterised using the approach described by Benbow and Bridgwater,[12] which is a development of that

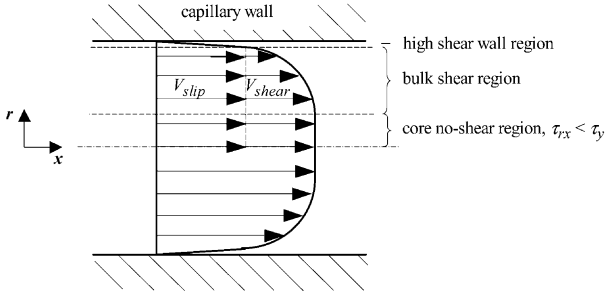

Fig. 3. Generalised capillary flow pattern.

of Oveston and Benbow[16] for the analysis of ceramics and clays undergoing extrusion. For flow through a die with dimensions shown in Fig. 2, the extrusion pressure is modelled as:

$$P = P_1 + P_2 = 2(\sigma_0 + \alpha V^m)\ln\left(\frac{D_0}{D}\right) + 4(\tau_0 + \beta V^n)\frac{L}{D} \quad (5)$$

where the velocity of the paste in the die land, V, is calculated by assuming that the paste is incompressible. The first term, P_1, describes the work done in the die entry region, based on an assumption of homogeneous deformation. It is not possible to associate a single shear rate with the die entry region, so an approximate ad hoc form of the Herschel–Bulkley constitutive equation has been used. Here σ_0 is a die entry yield term and α and m express the rate dependence, where the extrudate velocity is taken to be proportional to some sort of average shear rate. The term $(\sigma_0 + \alpha V^m)$ is known as the die entry yielding stress, Y:

$$Y = \sigma_0 + \alpha V^m \quad (6)$$

The second term, P_2, represents slip flow in the die land, ignoring any transients or entry effects. Eq. (5) has proved to be a good first order model for axisymmetric extrusion and provides reasonable design information, although the assumptions involved in the analysis makes its precision low. Further discussion of the applicability of Eq. (5) can be found in Blackburn et al.[17] As with capillary flow analysis, material parameters are obtained following a Bagley plot methodology, where the ordinate axis intercept yields P_1, to which values of the bulk yielding parameters may be fitted.

This paper reports on the use of both capillary and die entry flow analysis to characterise an industrial placebo paste, i.e. one without active ingredients, which are often present in small quantities. To ensure that the resulting material parameters may be used in further analysis of the extrusion-granulation process, the characterisation has been carried out over a suitably wide range of flow conditions and care has been taken to ensure that the parameters reliably reflect the variation of the characterisation data.

2. Methods and materials

The talc paste studied was based on an industrial formulation and its composition is summarised in Table 1.

2.1. Talc powder properties

Fig. 4 shows a scanning electron microscope (SEM, acquired on JSM-820, Jeol Ltd., UK) image of the talc powder. The particles are soft platelets, as indicated by the worn edges. It is difficult to obtain precise particle size distribution data for platelets since most available methods contain some uncertainty or assumptions over which dimensions of the platelets are measured. A particle size distribution obtained by laser diffraction (LS 200, Beckman Coulter, Inc., USA) measured all particles as having diameters between 1 and 20 μm in diameter, with a mean of 7μm. The material dimensions thus lie above the colloidal size range.

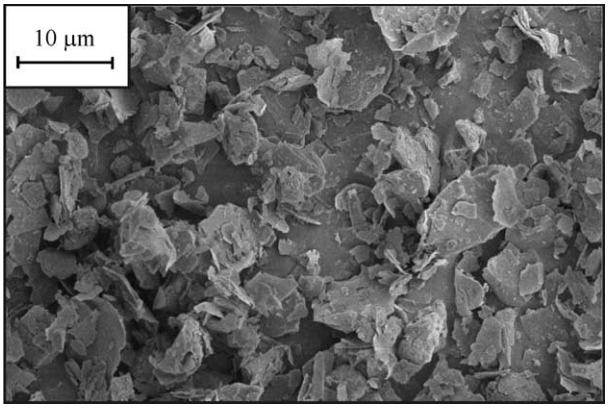

Fig. 4. SEM image of Micro-Talc AT Extra.

A very high voidage is possible when platelets are loose and randomly orientated, resulting in an order of magnitude difference between the actual particle density and the tamped apparent density. Uniaxial compaction experiments, using the ram extruder described in Section 1 with a blank replacing the die, were conducted in order to study the effect of stress on the voidage of the dry material. The barrel of 25.1 mm diameter, ~200 mm length and ~12 mm wall thickness was filled to its top by pouring in talc totalling 22.71 g (±0.01 g). The ram was lowered to compact the sample at a velocity of 0.5 mm/s until the force on the piston had reached its safe maximum limit of 50 kN, corresponding to a mean axial stress on the piston of ~100 MPa. The piston was then raised at a velocity of 0.1 mm/s until the sample had fully relaxed. The compacted talc density and voidage (calculated using particle density of 2.9 g/cm^3 quoted by the manufacturer) are presented in Fig. 5. The density increases from below 0.5 to above 2 g/cm^3. On relaxation, the compacted talc displayed a small elastic response, but the majority of the compaction was irreversible. The compacted plug was around 23 mm in height, similar to the barrel diameter. Wall shear stresses may have resulted in uneven compaction, although no evidence of this was observed.

2.2. Morwet solution properties

The surfactant powders contained significant amounts of absorbed water. Weighing samples of Morwet EFW and Morwet D425 powders before and after drying at

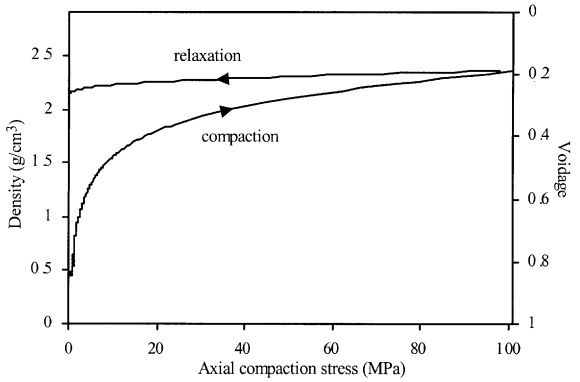

Fig. 5. Density and voidage of Micro-Talc AT Extra against compaction stress.

110 °C, indicated the absorbed water mass fractions of 0.097 and 0.059, respectively (calculated on a wet basis). Where solution concentrations have been calculated, the water absorbed in the powders has been included. The talc powder absorbed water mass fraction was only a fraction of one per cent, and was treated as negligible. The mass fraction of Morwet used in the paste liquid-phase was 0.392.

A solution with the composition given in Table 1 would be expected to lie well above the critical micelle concentration (CMC). Simple investigations into the physical properties of aqueous Morwet solutions prepared with the Morwet EFW to D425 ratio in Table 1 were conducted from surfactant mass fractions ranging from 0 to 0.5, above which solutions could not be successfully prepared. A concentric cylinder viscometer (LVDV-II +, Brookfield Engineering Laboratories, Inc., Stougton, MA, USA) was used with a low viscosity adapter to measure solution viscosities over the available range of shear rates at room temperature (recorded as 20.5 °C). An electronic balance and measuring cylinder were used to calculate the solution density. Apparent viscosity data for a 0.392 mass fraction solution over the available range of shear rates are presented in Fig. 6(a). No significant shear rate dependence is apparent over the shear rate range considered, and the mean value is 13.4 mPa s. The plot of mean viscosity against concentration in Fig. 6(b) indicates a CMC of ca. 0.3, above which the solution viscosity increases rapidly. The viscosity of the paste liquid-phase is therefore sensitive to the local Morwet concentration. The variation of solution density with concentration, shown in Fig. 6(c), appears to be linear: the density corresponding to the paste formulation is 1.16 g/cm^3.

2.3. Preparation of paste

Materials were weighed out on an electronic balance (LC 62105 or BA 6100 Sartorius balance, Sartorius Ltd., Edgewood, New York, USA). The dry talc and Morwet constituents were mixed in a planetary mixer (AE 200, Hobart Manufacturing Company Ltd., London, UK) for 30 min on speed setting one, stirring manually with a spatula every 5 min to displace any static material. Over the period between the fifteenth and twentieth minute the water was gradually poured into the dry mix. The resulting wet powder was then twice pugged through the mixer's mincer attachment at speed setting two. The final paste was left to relax in a hermetically sealed polythene bag for at least 2 h before use. Batches were always used within 36 h of preparation.

2.4. Experimental programme

Extrusion characterisation experiments were conducted using the ram arrangement illustrated in Fig. 2. The barrel, of diameter $D_0 = 25.1$ mm, was loaded with 140 g of paste for each extrusion, compacting manually with a rod to enable all of the paste to fit in the barrel. A screw action strain frame (SA100 Loading Frame, Dartec Ltd., Stourbridge, UK) was used to drive the ram and piston. The paste was precompacted with a force of 5 kN (corresponding to a mean axial stress of 10 MPa) applied for 5–10 s, which was considered to be sufficient to expel any entrained air. A plug of compacted paste approximately 140 mm in length was left in the barrel. The blank die was then replaced with the appropriate characterisation die. The piston was lowered to make contact with the paste plug with a force of 0.5 kN, and a 100 mm displacement characterisation run commenced. A PC running the software Dartec Workshop 95 was used to program a controller (Modular 9500 Digital Control System, Dartec Ltd., Stourbridge, UK) which regulated the strain frame's force, position and velocity. The controller recorded the force on the frame cross member and the cross member displacement against time. At least 220 force, displacement and time readings were recorded during each extrusion.

A total of 60 extrusion runs were carried out, in triplicate. To obtain useful capillary flow data it was necessary for the capillary length to diameter ratio, L/D, to be sufficiently large for flow in the capillary to become fully developed and entry and exit effects to become negligible. For reasons of practicality, sufficiently large length to diameter ratios could only be achieved for capillary diameters of 3 mm or less. Three such diameters were used, namely 1, 2 and 3 mm, where the L/D ratios varied from 2 to 16. Larger diameters (8, 15 and 20 mm) were used to provide further die entry pressure drop data, providing a total diameter reduction ratio, D_0/D, range from 1.3 to 25. Flow rates covering a mean extrudate velocity from 1.17 to 490 mm/s were studied, which covers the range of likely material velocities in an industrial extrusion-granulator.[6]

A number of piston velocities were used during the course of a single run, enabling a large number of velocities to be studied. The quality of extrusion pressure

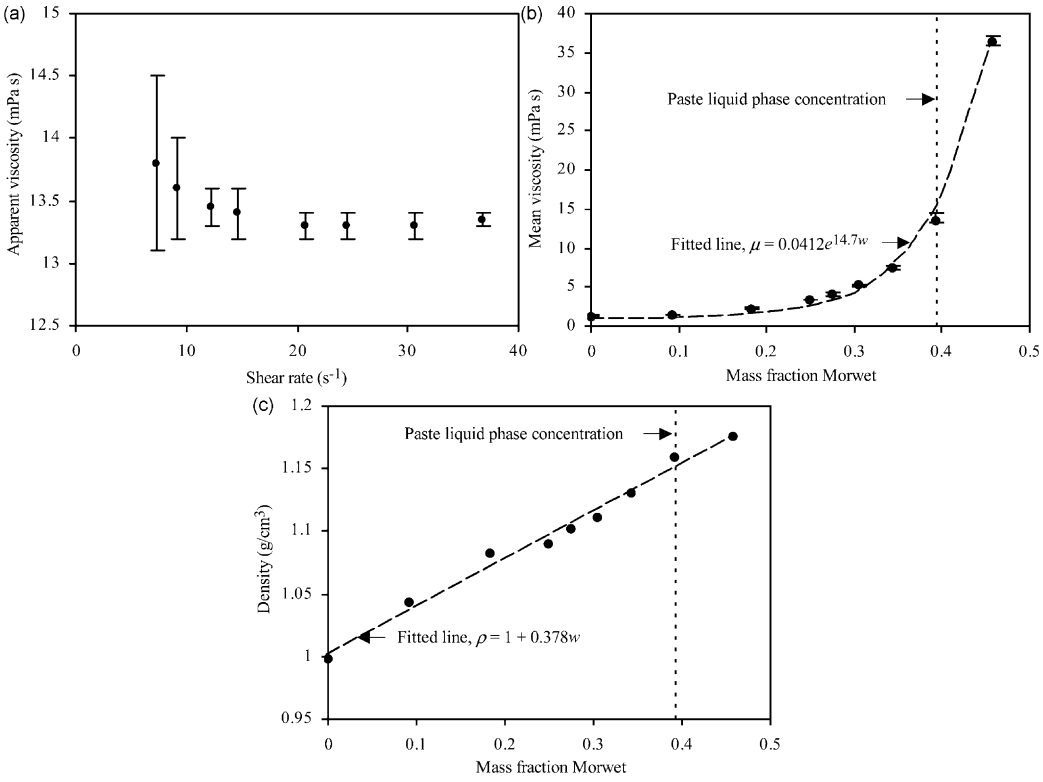

Fig. 6. Morwet solution properties. Error bars extend one standard deviation from mean. (a) Viscosity against shear rate, at solution mass fraction 0.392. (b) Mean viscosity against concentration, (c) Density against concentration.

data is compromised by this practice since the flow pattern and material changes occurring under one velocity may affect the flow pattern developed under the next. Where possible, the first velocity was repeated at the end of the sequence. For all 75 runs where this was done, the extrusion pressure for the repeated velocity was on average 8.4% less than for the first value, presumably due to the reduced frictional force at the barrel wall.

3. Results and analyses

3.1. General paste properties

The expected mass fraction of water in the paste, including the absorbed water in the Morwet, may be calculated as 0.178. The water content of triplicate samples from seven separate batches of paste prepared over the course of 2 months was measured by drying samples to constant mass under partial vacuum at 60 °C. These values ranged from 0.173 to 0.178, with a mean of 0.176, indicating that a small amount of liquid loss occurred during preparation. It seems reasonable to assume that the actual composition of the paste lay within 1–2% of the intended composition—although the sensitivity of the solution viscosity to concentration evident in Fig. 6(b) could render this variation significant.

The manufacturer's quoted talc particle density and the aqueous Morwet solution density from Fig. 6(c) enable the density of the paste, assuming no air entrainment, to be calculated as 2.02 g/cm^3. The liquid-phase volume fraction is expected to be 0.507. This voidage is noticeably larger than the void fractions of regularly packed mono-sized spheres (range 0.26–0.48)[18] and values reported for pastes containing near-spherical particles (near 0.40).[19]

A uniaxial compaction experiment, similar to that performed on the talc powder, was conducted on a sample of the paste. The compaction curves presented in Fig. 7 show that the measured density and voidage of

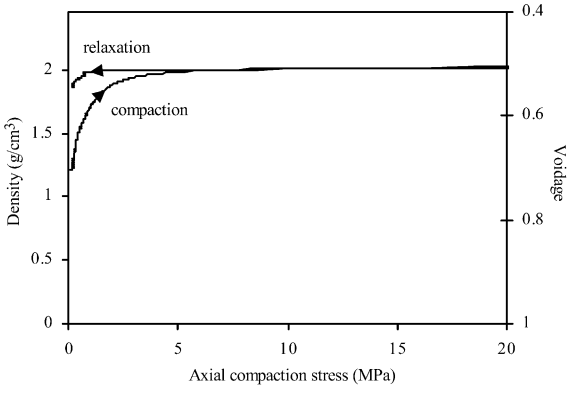

Fig. 7. Density and voidage of model paste against compaction stress.

the paste approach the predicted values. No liquid-phase was observed to escape during the compaction, so the increase in density was due to compression and expulsion of air entrained in the sample.

The high liquid-phase volume fraction meant that once the majority of the entrained air has been expelled, and after some rearrangement of the talc particles, the voids in the paste are likely to be saturated. The paste does not display the same change in density during compaction as the talc powder. Above a compressive stress of 5 MPa the paste can be assumed to be incompressible; the experimental protocol of precompacting paste to 10 MPa is well above that necessary to reach this limit. A little elasticity of the sample is apparent; this may be due to compression of entrained air or particle elasticity. The bulk of the compression was irreversible, with the post-compression sample having a density of 1.9 g/cm^3.

A length of extrudate from a typical run ($D=3$ mm, $L=48$ mm, $V_p=2$ mm/s) was allowed to dry, then snapped such that a fracture surface was exposed on the cross section. An environmental scanning electron microscope (ESEM, acquired on JSM-5600LV, Jeol Ltd., UK) image of a region of this cross section is shown in Fig. 8. The densely packed platelets are visible in this image, and no pockets of entrained gas are apparent. The complex microstructure formed by the various platelet orientation is also visible.

3.2. Phase migration and dilation

As a paste flows its structure will change. Two effects are of particular importance; the pressure gradients in the paste may cause the liquid-phase to migrate, and a compacted material forced to flow will dilate as particles re-arrange to move over one another. A sample extrusion run was conducted to ascertain how significant these effects are.

To maximise any phase migration a long die was chosen to increase the extrusion pressure ($D=3$ mm, $L/D=16$); a low piston velocity ($V_p=0.05$ mm/s) was chosen to allow the liquid-phase more time to migrate.[20] Samples of extrudate were collected over the course of the test and their densities calculated through measurements of mass and geometry. Once the extrusion was complete, the remaining plug of paste in the barrel was removed and sliced into 10 mm thick sections which were also analysed for density and water content.

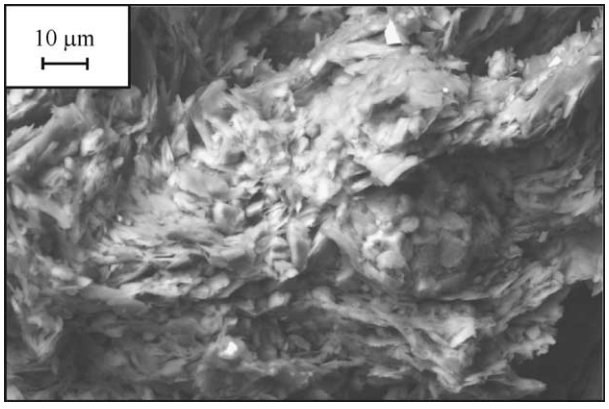

Fig. 8. ESEM image of dried extrudate cross section. $D=3$ mm, $L=48$ mm, $V_p=2$ mm/s.

The extrusion pressure profile over time is presented in Fig. 9(a). The profile can be divided into three flow regions; (1) compaction; (2) transient; and (3) steady state. Over the compaction region entrained air in the paste is expelled until the extrusion pressure rises very rapidly and reaches a peak, at which point flow commences. Immediately after flow has commenced there is a transient period, after which some optimal flow pattern is reached and the rest of the extrusion run proceeds at a nominal steady state value of 7 MPa. Inhomogeneity in the paste (e.g. air bubbles or agglomerates) can lead to fluctuations and spikes in the steady state extrusion pressure. The extrusion pressure is generally constant over time, indicating that it is insensitive to any physical change in the paste in the barrel over the course of the run.

It is apparent in Fig. 9(b) that both the extrudate density and liquid content differ from their nominal values in a uniform manner, possibly through a combination of dilatancy and liquid-phase migration. This is in general agreement with other studies of liquid-phase migration where the extrudate is, at least initially, found to be wetter than expected, but the associated change in density is not commonly reported.[20,21] Fig. 9(c) shows that the density and water content vary over the length of the barrel plug. Liquid-phase has migrated from material in the barrel to the extrudate, leaving the plug with a lower liquid content, with consequent effect on the plug density.

Incorporating these density effects into any rheological characterisation poses considerable difficulty, and would increase the complexity of the model significantly. The extrusion pressure and extrudate properties remained constant throughout the extrusion run—so the run can still be considered as steady state flow. The characterisation proceeds with the assumption of a homogeneous material, but with the recognition that the flowing density differs from the formulated one. This has not been reported previously, and the consequences in terms of the actual versus assumed extrudate velocity have not been assessed.

3.3. Capillary flow

The extrusion pressure profiles over time show noticeable transients when the piston velocity is changed, presumably due to a combination of machine adjustment, elastic effects and changes in flow pattern.

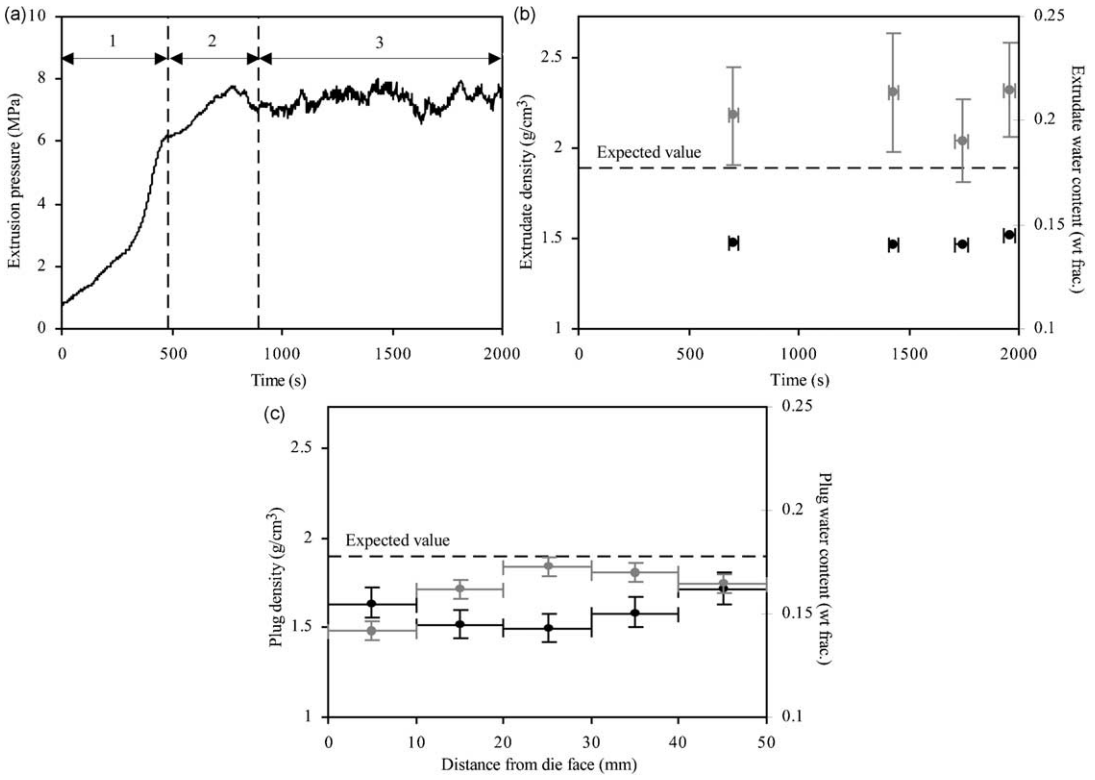

Fig. 9. Density and water content variation over a sample ram extrusion run. $D = 3$ mm, $L/D = 16$, $V_p = 0.05$ mm/s. (●) density, (●) water content. Error bars bound regions of possible values. (a) Extrusion pressure against time. (b) Relaxed extrudate properties against time. (c) Relaxed barrel plug properties against position.

These transients are more significant for the runs with smaller area reduction. This is most likely because the ratio of the volume of paste in the barrel and the volume of paste in the die land decreases as the area reduction is decreased, for a constant barrel diameter. Thus the effective duration of the experiments is shortened, and the transients become more dominant. A steady state is reached so long as the extrusion period is sufficiently long, and the mean value of extrusion pressure in these steady regions is used for the analysis.

Forty-five Bagley plots were constructed in order to find the wall shear stresses and die entry pressures for each of the six capillary diameters using all of the piston velocities (flow rates) used. Two sample plots are presented in Fig. 10). Both show a linear relationship between the extrusion pressure and L/D, which suggests that the wall shear stress is not a function of the normal stress on the wall.

It is clear that the reproducibility between independent runs is poor, with variation up to 50% in the data for the $D = 15$ mm case. This problem was most apparent with the larger capillaries, where the capillary diameter approached the barrel diameter. As noted above, longer periods are required at each velocity for steady state to be reached with these diameters. It is acknowledged in the following analysis that the compromise between the quality of the extrusion pressure data and the number of piston velocities may have been weighted too far towards maximising the number of piston velocities.

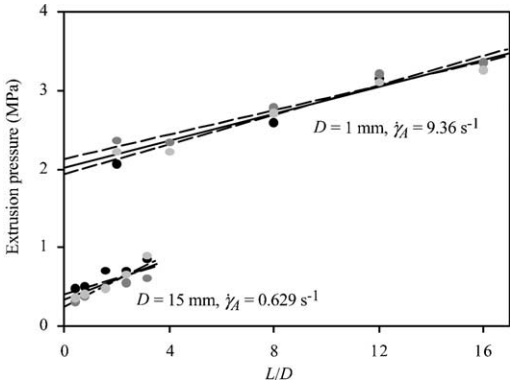

Fig. 10. Bagley plots of extrusion pressure against capillary length to diameter ratio; $V = 0.00117$ m/s. (●) (●) (●) independent sets of data, (—) least squares fit, (– –) boundary least squares fit.

Linear regression of the data allowed wall shear stresses and die entry pressures to be estimated. The variation in reproducibility of the data was quantified by setting boundaries to what the 'best' linear fit might be. If statistical information about the data were available, then exact probability distributions for the fit parameters might be calculated. Rather, a novel approach was used where the square of the coefficient of correlation (often known as R^2) was taken to be an

indicator of the quality of the data. Regression parameters were then obtained which gave a squared coefficient of correlation equal to the original raised to the power of 1.3. This index was chosen arbitrarily to give fitted lines which appeared reasonable. The least squares and the boundary fits are shown in Fig. 10, and it can be seen that the boundaries of the ordinate intercepts and gradients would seem to cover all linear fits which might be deemed reasonable. Reproducibility of paste extrusion data has been reported previously to be poor, with a repetition reproducibility of 10% suggested.[22]

An example set of wall shear stress data, for the case $D = 1$ mm, is presented in Fig. 11 against the mean axial velocity. The resultant Mooney plots presented in Fig. 12 show an apparently non-linear relationship between the apparent shear rate and $8/D$. Although a straight line could be fitted to these data with a gradient of the slip velocity, the line would intercept the ordinate axis at a negative value which, considering Eq. (4), is not consistent with the physical model presented. Thus no conclusions about the nature of the flow can be drawn from these Mooney plots.

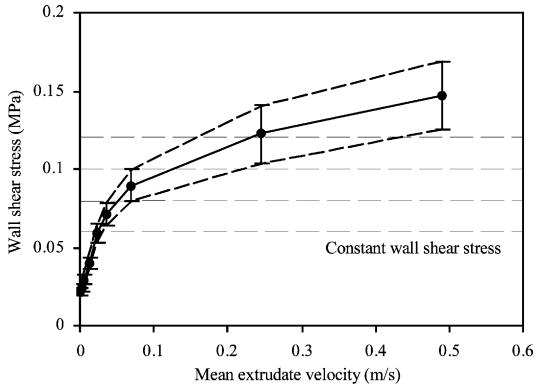

Fig. 11. Wall shear stress against mean extrudate velocity $D = 1$ mm. Error bars bound regions of possible values. (—) interpolated most likely value, (– –) interpolated boundary value.

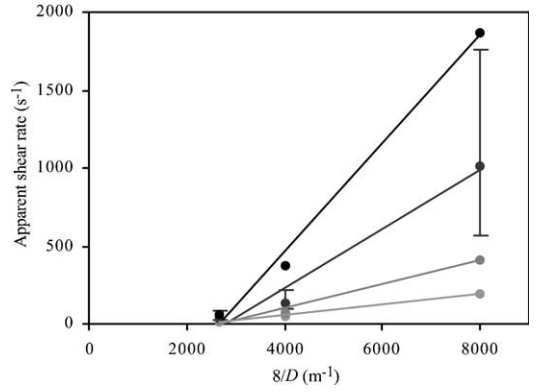

Fig. 12. Mooney plot of apparent shear rate against $8/D$. τ_w=(●) 0.12 MPa, (●) 0.10 MPa, (●) 0.08 MPa, (●) 0.06 MPa. (—) least squares fits. Selected error bars bound regions of possible values.

Successful attempts to find slip velocities using Mooney plots have previously been reported for pastes such as soap, alumina/water catalyst greens and ammonium sulphate/polymeric liquid paste.[22,23] However, other physically unrealistic cases have been reported, notably by Jastrzebski[24] for kaolinite pastes. He reported the empirical result that wall shear stress against wall slip velocity data over a range of capillary diameters aligned on the same curve when the wall slip velocity was divided by the diameter, but offered no physical justification this feature. He wrote the corresponding interface layer condition as:

$$\tau_w = \beta_c V_{\text{slip}} D \tag{7}$$

Substituting this into Eq. (4) gives,

$$\frac{32Q}{\pi D^3} = \frac{8}{D^2}\frac{\tau_w}{\beta_c} + \frac{4}{\tau_w^3}\int_{\tau_y}^{\tau_w}\left(\frac{\tau - \tau_y}{K}\right)^{1/\lambda}\tau^2 \mathrm{d}\tau \tag{8}$$

A plot of the apparent shear rate against $8/D^2$, at constant wall shear stress, should be linear and the parameter β_c may be calculated from the gradient. Jastrzebski found β_c to vary with wall shear stress, and suggested that it was dependent on suspension microstructure. This interface layer condition has become a common fall back for studies where Mooney analyses have yielded unrealistic results. Adams et al.[25] studied a clay/oil paste and reported Mooney plots with negative ordinate axis intercepts, whilst Khan et al.[26] studied an alumina/polymer paste and reported plots indicating slip velocities greater than the mean extrudate velocity. Use of the Jastrzebski type interface layer condition yielded apparently sensible results in both cases, with Adams et al. finding β_c to increase linearly with wall shear stress.

Mooney diagrams based on the Jastrzebski interface layer condition for the talc paste are presented in Fig. 13. Linear least squares fits, forced to pass through the origin (implying plug flow in the capillary), were applied to these data and appear plausible. Fig. 14

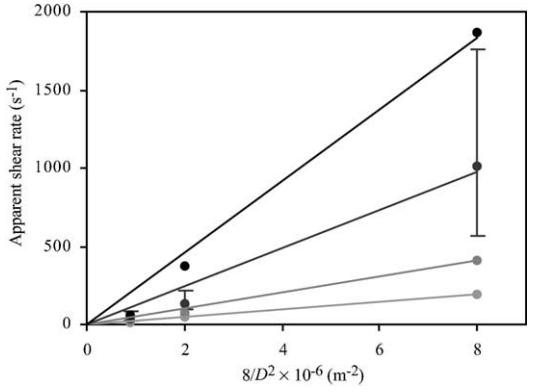

Fig. 13. Apparent shear rate against $8/D^2$. τ_w=(●) 0.12 MPa, (●) 0.10 MPa, (●) 0.08 MPa, (●) 0.06 MPa. (—) least squares fits. Selected error bars bound regions of possible values.

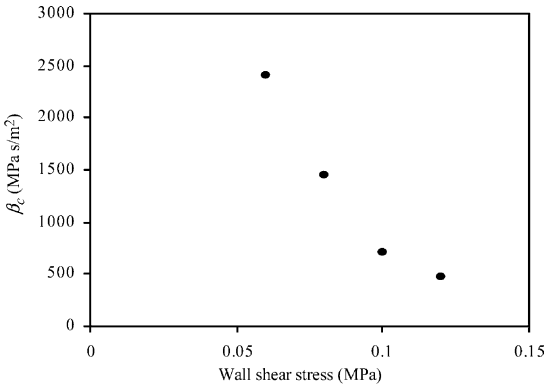

Fig. 14. Jastrzebski interface layer condition: variation of β_c against wall shear stress.

shows that the β_c term decreases as the wall shear stress increases.

The value of the Jastrzebski parameter is limited, both because the physical basis for inclusion of the diameter is unknown, and its extension to non-cylindrical ducts is thereby unresolved. In those cases where it has been reported, the β_c term is itself dependent on the wall shear stress, thus the actual form of Eq. (7) is more complex and varies case by case.[24,25]

In Fig. 15, the wall shear stress is presented against both the apparent shear rate and the mean extrudate velocity. If there were no wall slip, then the wall shear stress would be a function of the apparent shear rate only, whereas if there were total wall slip then it would be a function of mean extrudate velocity only. The flow curves for the three capillary diameters do not collapse onto a single curve on either plot—thus indicating a combination of wall slip and shearing (contrary to the results of the Jastrzebski analysis which suggested total slip). Resolution of the two components requires identification of the wall slip velocity, but as has been seen, there is uncertainty over the validity of the values obtained.

Where capillary flow experiments yield successful Mooney diagrams, the paste could be considered as 'well-behaved'. Where materials are thought to be slipping and shearing, but which give unsuccessful Mooney diagrams, such as the talc paste presented here, the paste could be considered as 'badly-behaved'. However, such materials must still be characterised in order to make process predictions. In this case it was thought simplest to assume that the paste undergoes plug flow with total wall slip, but for use in process models the errors associated with this assumption must be bounded.

Material parameters for the interface layer condition presented in Eq. (3) were obtained by a least-squares fit through the combined data sets for $D = 1$, 2 and 3 mm. The spread of the data was taken into account by fitting

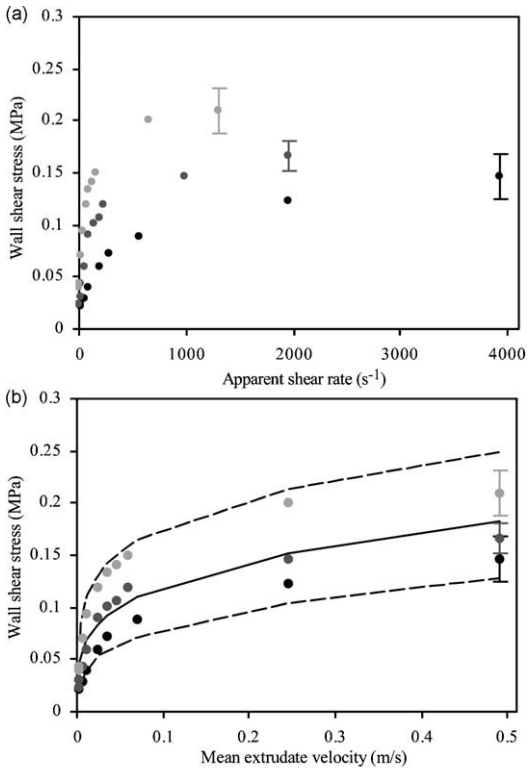

Fig. 15. Wall shear stress against apparent shear rate and mean extrudate velocity. Selected error bars bound regions of possible values. $D = ($●$)$ 1 mm, $($●$)$ 2 mm, $($●$)$ 3 mm. (—) least squares fit, (– –) boundary least squares fit. (a) Apparent shear rate, (b) Mean extrudate velocity.

lower and upper bounds to the parameters. The lower bound parameters were found by a least squares fit through the lower error boundary values for the $D = 1$ mm capillary. Upper bound parameters were obtained by a least squares fit through the upper boundary data similarly for the $D = 3$ mm capillary. These parameter fits are shown in Fig. 15(b), and the parameters generated are listed in Table 2.

The wall shear stress shows a strong rate dependence, with a shear thinning behaviour. At mean extrudate velocities over around 0.2 m/s, the stress is practically constant at around 0.15 MPa. Below 0.2 m/s, the wall shear stress decreases towards zero; thus the best parameter fits were achieved with zero yield stress (where $\tau_0 = 0$). The viscosity measurements indicated that the liquid-phase was Newtonian, with no apparent yield stress: these liquid-phase characteristics are consistent with the absence of an interface layer yield stress. This is not unexpected as the solids volume fraction is not high, thus the frictional interactions of the solid matrix contacts with the wall would not be significant. The non-linear rate dependency does not follow directly from the liquid-phase properties; particle interactions and changes in the interface layer conditions must play a part.

Table 2
Model paste constitutive parameters

Parameter	Best fit	Lower bound	Upper bound
σ_0, MPa	0.15	0.19	(0)
α, MPa (m/s)$^{-m}$	1.0	0.78	1.3
m	0.23	0.57	0.10
τ_0, MPa	(0)	(0)	(0)
β, MPa (m/s)$^{-n}$	0.22	0.16	0.29
n	0.26	0.3	0.21

Parameters were forced to be non-negative.

3.4. Die entry

Capillary flow analysis did not yield information about the bulk shearing or extensional properties of the paste. The die entry extrusion pressures obtained from Bagley plots, such as those in Fig. 10, have been analysed using Eq. (5).

The variation of the die entry yielding stress with mean extrudate velocity is presented in Fig. 16(a). The data from the different capillary diameters do not lie on a single curve. This could be related to the problems associated with using the mean extrudate velocity as the rate term, as has been previously reported.[17,27] The same data are presented against V/D, a term proportional to the apparent shear stress in the capillary, in Fig. 16(b), but the curves do not lie any closer together in this case. Dimensional analysis of the system indicates that the die entry yielding stress is likely to be a function of both V/D and D_0/D, however inspection of the data did not indicate any dependency of this nature.

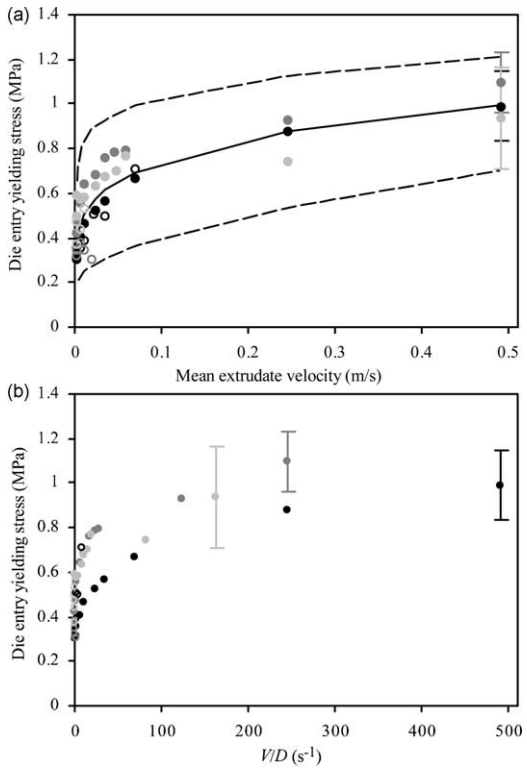

Fig. 16. Die entry yielding stress against extrudate velocity and velocity to diameter ratio. Selected error bars bound regions of possible values. D = (●) 1 mm, (●) 2 mm, (●) 3 mm, (○) 8 mm, (○) 15 mm, (○) 20 mm. (—) least squares fit, (– –) boundary least squares fit. (a) Extrudate velocity, (b) Ratio of extrudate velocity to capillary diameter.

The die entry yielding stress appears to follow a power law relationship when plotted against the mean extrudate velocity, possibly with an apparent yield stress (that is, a non-zero ordinate intercept). The three parameter model from Eq. (5) was used. The same approach as in Section 3.3, of using best fit parameters, was used in estimating the model parameters and the results are presented in Table 2.

The die entry yielding stress shows a strong rate dependence, with shear thinning behaviour. As with the wall interface layer condition, at mean extrudate velocities over around 0.2 m/s, the stress is practically constant, with a value around 0.8 MPa. In this range the paste might be considered as a perfect plastic. Below 0.2 m/s, the wall shear stress decreases, very rapidly so below 0.05 m/s. The lower bound and the best fit parameter groups show the yielding stress intercepting the ordinate axis at a positive value, indicating a yield stress. However, the gradient is too steep for these yield stress values to be quoted with much confidence. The boundary parameter fits extend very widely over the data, with the velocity index m varying by over a factor of 2. The boundaries could be tightened, but at the expense of their confidence.

4. Discussion and conclusions

The talc paste has proved difficult to characterise rigorously. This reflects the choice of an industrially relevant paste over a wide range of flow conditions, rather than a paste designed to be well-behaved over a small range of conditions. Experimental difficulties were found achieving reproducible extrusion pressures, which is common for most pastes.[22] Investigation of the paste consistency suggested that little variation occurred between batches, although the viscosity of the Morwet solution was found to be very sensitive to concentration in the range used. Improvement of the extrusion pressure data quality might be achieved without increased experimental work by reducing the number of piston velocities used per run, and basing the characterisation on fewer velocities.

A best fit and bounding approach has been developed to provide useful characterisation parameters for this badly-behaved paste. The experimental and fitted model extrusion pressures are compared in Fig. 17. The root-mean-square normalised error over all the best fit parameter data points is 0.22. The boundary parameter predictions successfully bound the experimental values,

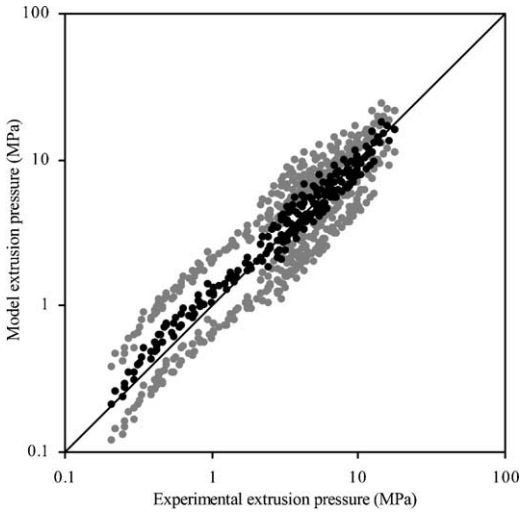

Fig. 17. Model against experimental extrusion pressure. (●) best fit parameters, (●) boundary parameters.

but in most cases deviate substantially from it. This characterisation method provides a simple and industrially relevant model of the material, but the accuracy of predicted experimental extrusion pressures in axisymmetric systems should not be expected to be better than around 20%, which compares to an experimental reproducibility of around 10%.[22]

The paste characterisation has included studies of the talc particle size distribution, the liquid-phase rheology, liquid-phase migration, paste dilatancy, paste wall slip during capillary flow, and paste flow into a die entry. With the formulation used, the talc platelet shape and the high liquid fraction combine to give a paste with a relatively low solids volume. Under a compaction stress of over 5 MPa the voidage becomes totally saturated with liquid-phase, and has a voidage of 0.51. The high liquid-phase fraction reflects the ease of processing and final dispersion property requirements of the industrial material.

A higher solids fraction tends to cause a paste to display more plastic characteristics, such as little rate dependence and an apparent yield stress.[12] It follows that the low solids faction of the talc paste causes significant rate dependence, with no clear apparent yield stress, which complicates its characterisation. The low solids fraction is also a factor contributing towards the observed phase migration. Whether, or not, phase migration is significant in a particular system will be dependent of the pressure gradients and time scales involved, and must be considered on a case by case basis.

A two-phase particle/liquid model is often used in the study of soil mechanics,[28] and has occasionally been applied to pastes.[29,30] The liquid-phase is characterised as having a pore pressure, and the solid-phase as carrying an effective stress. The total stress is the sum of the pore pressure and the effective stress. The talc paste features a high liquid-phase fraction; following the application of a total stress, at least initially, a substantial fraction of the total is carried by the pore pressure. Thus, it is likely that the talc paste exhibits largely isotropic behaviour, although this has not been successfully tested.

Migration of the liquid-phase towards the walls is thought to account for a high shear wall region, which causes the apparent paste wall slip.[10,11] The capillary analysis flow curves in Fig. 15 did not align when plotted against either the mean velocity (indicating plug flow) or the apparent shear rate (indicating no wall slip). Either a combination of wall slip and bulk shearing is occurring, or there is systematic error with the data. A Mooney analysis of the data yielded plots which were not physically plausible (an ordinate axis intercept indicating a negative contribution to flow due to bulk shearing). Using the Jastrzebski interface layer condition appeared to yield plausible results (although it indicated plug flow, contrary to the lie of the flow curves), but only offers a material parameter which varies with the wall shear stress and which cannot be applied to non-cylindrical geometries.

Previous studies known to the authors which have discussed similar problems with the Mooney analysis either suggest that experimental error was responsible,[31] or resort to using the Jastrzebski interface layer condition.[24,25,26] A simple understanding of the problem can be gained by considering microstructural changes in the paste during extrusion. The Weissenberg–Rabinowitsch Eq. (4) is derived assuming constant constitutive equation parameters throughout the material. It is possible that the microstructure of many paste materials will change during flow, and quite possibly across the cross section of the capillary. This is especially so for the talc paste, where platelet orientation leads to structure as seen in Fig. 8. If this is so, the constitutive parameters will vary correspondingly over the diameter of the capillary. Thus, the second term on the right hand side of Eq. (4) may not be constant over the $8/D$ range, and the Mooney analysis will fall down. In such cases, it may still be possible to find some interface relationship which yields apparently viable Mooney plots (e.g. the Jastrzebski condition) but there would be no grounds to believe that the plots provide true values of wall slip.

Where this is the case, other methods of determining the extent of wall slip during capillary flow might be employed, although they were not attempted as part of this study. Two standard techniques are to use colour marking[32] and to use roughened dies.[33] Colour marking requires a plug of coloured paste (otherwise identical to the normal paste) to enter the die mid flow. Analysis of the shape of the plug exiting the die enables the relative amounts of bulk shear and wall slip to be determined. Roughened die surfaces could be used in an attempt to eliminate wall slip. The amount of wall slip in the normal

case may be found by comparison to the no-slip case. However, both of these techniques involve an increased degree of experimental complexity, and are not without their own difficulties.

Attempts to directly observe an interface layer using particles large enough to be conventionally photographed have been largely unsuccessful.[34] Studies using Magnetic Resonance Imaging[35] report being able to detect an increase in liquid-phase next to the wall, however, the imaging resolution was not sufficient to obtain any detailed information about the concentrations. Some promising work has been reported using infrared spectroscopy,[36] where an apparent decrease in concentration next to the wall for a system of ethylcellulose particles in aqueous solution was measured. An alternative methodology is the use of Discrete Element Simulations (DEM) of individual particle–particle interactions in such systems. Simulations of wall layers in less dense suspensions have clearly indicated the reorientation of non-spherical particles under shear near the wall.[37]

Despite the efforts made to characterise the talc paste over a range of conditions applicable to the industrial production of WDGs, the badly-behaved nature of the paste limits the confidence of the material parameters found. The adopted approach of using bounding parameters gives an indication of the confidence, but will not be a substitute for appropriate scale up work. Further experiments using colour marking or roughened die techniques could yield a more complete picture of the interface behaviour, and help to develop a more complete material characterisation.

Acknowledgements

The authors gratefully acknowledge support from Syngenta and the Engineering and Physical Sciences Research Council (UK), along with the help of Dr. S. Rough, of Cambridge University, and Mr. I. Wratten, of Syngenta, in obtaining extrudate images. PJM also acknowledges the support of an ICI PhD scholarship.

References

1. Das, R. N., Madhusoodana, C. D. and Okada, K., Rheological studies on cordierite honeycomb extrusion. *J. Eur. Ceram. Soc.*, 2002, **22**(16), 2893–2900.
2. Agote, I., Odriozola, A., Gutierrez, N., Santamaria, A., Quintanilla, J., Coupelle, P. and Soares, J., Rheological study of waste porcelain feedstocks for injection moulding. *J. Eur. Ceram. Soc.*, 2001, **21**(16), 2843–2853.
3. Özkan, N., Oysu, C., Briscoe, B. J. and Aydin, I., Rheological analysis of ceramic pastes. *J. Eur. Ceram. Soc.*, 1999, **19**(16), 2883–2891.
4. Dubus, M. and Burlet, H., Rheological behaviour of a polymer ceramic blend. *J. Eur. Ceram. Soc.*, 1997, **17**(2–3), 191–196.
5. Zhou, Y. X. and Mallick, P. K., Effects of temperature and strain rate on the tensile behavior of unfilled and talc-filled polypropylene. Part I: Experiments. *Polymer Eng. Sci.*, 2002, **42**(12), 2449–2460.
6. Martin, P. J., Mechanics of Paste Flow in Radial Screen Extruders. PhD Thesis, University of Cambridge, UK, 2002.
7. Lyne, C. W. and Johnston, H. G., The selection of pelletisers. *Powder Techn.*, 1981, **29**, 211–216.
8. Leuenberger, H., Monitoring granulation. *Manufacturing Chemist*, 1984, **55**(5), 67–71.
9. Herschel, W. H. and Bulkley, R., Measurement of consistency as applied to rubber-benzene solutions. *Proc. Am. Soc. Testing Materials*, 1926, **26**(2), 621–633.
10. Leighton, D. and Acrivos, A., The shear-induced migration of particles in concentrated suspensions. *J. Fluid Mech.*, 1987, **181**, 415–439.
11. Yilmazer, U. and Kalyon, D. M., Dilatancy of concentrated suspensions with Newtonian matrices. *Polymer Composites*, 1991, **12**(4), 226–232.
12. Benbow, J. and Bridgwater, J., *Paste Flow and Extrusion*. Clarendon Press, Oxford, UK, 1993.
13. Rabinowitsch, B., Über die Viskosität und Elastizität von Solen. *Zeitschrift für Physikalische Chemie—Abteilung A*, 1929, **145**, 1–26.
14. Mooney, M., Explicit formulas for slip and fluidity. *J. Rheology*, 1931, **30**, 210–222.
15. Bagley, E. B., End corrections in the capillary flow of polyethylene. *J. Appl. Phys.*, 1957, **28**, 624–627.
16. Oveston, A. and Benbow, J. J., Effects of die geometry on the extrusion of clay-like material. *Trans. British Ceram. Soc.*, 1968, **67**, 543–567.
17. Blackburn, S., Burbidge, A. S. and Mills, H., A critical assessment of the Benbow approach to describing the extrusion of highly concentrated particulate suspensions and pastes. In *Proceedings of the XIIIth International Congress on Rheology*. Cambridge, UK, 2000.
18. Furnas, C. C., Grading aggregates I: Mathematical relations for beds of broken solids of maximum density. *Industrial and Engineering Chemistry*, 1939, **23**(9), 1052–1058.
19. Yilmazer, U. and Kalyon, D. M., Slip effects in capillary and parallel disk torsional flows of highly filled suspensions. *J. Rheology*, 1989, **33**(8), 1197–1212.
20. Rough, S. L., Bridgwater, J. and Wilson, D. I., Effects of liquid phase migration on extrusion of microcrystalline cellulose pastes. *Int. J. Pharmaceutics*, 2000, **204**, 117–126.
21. Tomer, G. and Newton, J. M., Water movement evaluation during extrusion of wet powder masses by collecting extrudate fractions. *Int. J. Pharmaceutics*, 1999, **182**, 71–77.
22. Amarasinghe, A. D. U. S., Interpretation of Paste Extrusion Data. PhD Thesis, University of Cambridge, UK, 1998.
23. Yilmazer, U. and Kalyon, D. M., Dilatancy of concentrated suspensions with Newtonian matrices. *Polymer Composites*, 1991, **12**(4), 226–232.
24. Jastrzebski, Z. D., Entrance effects and wall effects in an extrusion rheometer during the flow of concentrated suspensions. *Industrial and Engineering Chemistry Fundamentals*, 1967, **6**(3), 445–454.
25. Adams, M. J., Briscoe, B. J. and Sinha, S. K., Interfacial and bulk rheological characterisations of paste materials in extrusion flow. In *27th International SAMPE Technical Conference*, 9/12/1995.
26. Khan, A. U., Briscoe, B. J. and Luckman, P. F., Evaluation of slip in capillary extrusion of ceramic pastes. *J. Eur. Ceram. Soc.*, 2001, **21**(4), 483–491.
27. Zheng, J., Carlson, W. B. and Reed, J. S., Flow mechanics on extrusion through a square-entry die. *J. Am. Ceram. Soc.*, 1992, **75**(11), 3011–3016.
28. Atkinson, J. H., *An Introduction to the Mechanics of Soils and Foundations*. McGraw-Hill, Maidenhead, UK, 1993.

29. Burbidge, A. S., Bridgwater, J. and Saracevic, Z., Liquid phase migration in paste extrusion. *Trans. Inst. Chemical Engineers, Part A (Chemical Engineering Research and Design)*, 1995, **73**, 810–816.
30. Poitou, A., Racineux, G. and Burlion, N., Identification and measurement of pastes rheological properties—effects of water dissociation. *Water Science and Technology*, 1997, **36**(11), 19–26.
31. Corfield, G. M., Adams, M. J., Briscoe, B. J., Fryer, P. J. and Lawrence, C. J., A critical examination of capillary rheometry for foods (exhibiting wall slip). *Trans. Inst. Chemical Engineers, Part C (Food and Bioproducts Processing)*, 1999, **77**(1), 3–10.
32. Graczyk, J., Gonzalez-Alvarez, A., Arellano, M. and Buggisch, H., Characterisation of wall slip in extrusion of ceramic pastes. *Euro Ceramics vii, Pt 1-3*, 2002, **206–213**, 321–324.
33. Halliday, P. J. and Smith, A. C., Compaction and flow of potato starch and potato granules. *Food Sci. and Technology Int.*, 1997, **3**, 333–342.
34. Lukner, R. B. and Bonnecaze, R. T., Piston-driven flow of highly concentrated suspensions. *J. Rheology*, 1999, **43**(3), 735–751.
35. Modigell, M., Hufschmidt, M., Koke, J., Heine, C., Han, S., Stapf, S. and Petera, J., Investigation of wall slippage in suspensions by NMR imaging. In *Proceedings of the XIIIth International Congress on Rheology*. Cambridge, UK, 2000, 4-175–177.
36. Tuchinda, P., Hartman Kok, P. J. A., Kazarian, S. G., Lawrence, C. J. and Briscoe, B. J., *Rheological Methods in Food Process Engineering*. Freeman Press, East Lansing, MI, USA, 2001.
37. Pozrikidis, C., Dynamical simulation of the flow of suspensions: wall-bounded and pressure-driven channel flow. *Industrial and Engineering Chemistry Res.*, 2002, **41**, 6312–6322.